Food Chemistry: X 25 (2025) 102165

Contents lists available at ScienceDirect

Food Chemistry: X

journal homepage: www.sciencedirect.com/journal/food-chemistry-x

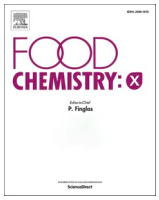

Comparing parboiling and milling for selenium-enriched rice (*Oryza sativa L.*): Differences in selenium speciation, texture, microstructure, and sensory

Kun Zhuang [a,*,1], Zihan Zhang [a,1], Shuyou Shang [a], Kai Zheng [a], Xiaolong Zhou [b], Wenjing Huang [a], Yuehui Wang [b,c], Wenping Ding [a,*]

[a] *Key Laboratory of Bulk Grain and Oil Deep Processing (Ministry of Education), Department of Food Science and Engineering, Wuhan Polytechnic University, Wuhan 430023, China*

[b] *College of Modern Industry of Selenium Science and Engineering, Wuhan Polytechnic University, Wuhan 430023, China*

[c] *National Selenium-Rich Agricultural Products Processing Technology Research and Development Center, Wuhan 430023, China*

ARTICLE INFO

Keywords:
Selenium-enriched rice
Parboiled rice
SEM
CLSM
Electronic tongue
Electronic nose

ABSTRACT

Parboiled rice can effectively retain Se during milling. In this study, Se-enriched rice grains were sprayed with three different concentrations of bioSeNPs fertilizer on the leaves at heading stage and then processed into parboiled and milled rice. The aim was to investigate the effects of parboiling on Se speciation, texture, microstructure, taste, and flavor of cooked rice. The results showed that parboiling enhances the total Se content by making the bran more difficult to remove. At milling for 40 s, selenomethionine (72.6 %–80.1 %) is predominant Se speciation. Parboiled rice exhibited higher hardness, reduced stickiness, with only minor differences in chewiness. The results regarding cooking quality and microstructure indicated that parboiling restricts starch dissolution during cooking, while the protein remains distributed within starch cell gaps. The parboiling enhances umami and flavor while maintaining the original taste and flavor profile. This work provides valuable insights for application of Se-enriched rice in parboiled rice.

1. Introduction

Multiple studies confirm selenium's (Se) multifaceted health benefits, including anti-cancer, antioxidant, and immune-modulating effects, as well as its ability to lower blood sugar levels. (Farooq, Zhang, Liu, et al., 2024). Statistics indicate that the Se intake among Chinese residents ranges from 26 to 32 μg/d, which falls short of the recommended daily intake of 60 to 400 μg/d for adults (Farooq, Zhang, Yuan, et al., 2024). Therefore, it is crucial to develop safe and nutritious selenium-rich foods derived from plant, animal, and microbial sources to address the needs of populations in Se-deficient regions. Plants are capable of metabolizing inorganic Se into organic forms. Relevant research suggests that the bioavailability of Se in Se-enriched crops is greater than that found in Se-enriched animal products (White, 2018). Furthermore, the application of Se fertilizer during crop cultivation results in agricultural products, including cereals, vegetables, and soybeans, containing over 50 % organic-Se (Muleya et al., 2021).

Cereals serve as a staple food and are the primary source of Se intake for individuals following low-protein diets. They also play a significant role in the composition of Se-enriched foods (Huang et al., 2018). Research indicates that rice possesses a strong capacity for Se enrichment, typically achieved through the application of Se fertilizers to the soil and the foliar spraying of Se biological agents (Xiong et al., 2023). Among Se-enriched rice, bran contains the highest Se concentration, exceeding that of the grains by more than twofold. Approximately 13.7 % of Se is lost during the rice milling process (Shen et al., 2019). Liu et al. (2009) observed that as the grinding accuracy increased from 2.71 % to 17.96 %, the Se loss rate escalated from 6.51 % to 34.28 %.

Parboiled rice is a novel variety of rice that undergoes three processing stages: soaking, parboiling, and drying (Muchlisyiyah et al., 2023). During the soaking phase, certain water-soluble nutrients are transferred from the aleurone layer of brown rice to the endosperm (Balbinoti et al., 2018). Research has indicated that parboiled rice is more nutritious than milled rice (Wu et al., 2023). This characteristic may contribute positively to minimizing selenium loss during the milling process; however, there is currently a lack of systematic studies to verify this claim. Saha and Roy (2020) reviewed reports on the incorporation of elements such as calcium, iron, and zinc to enhance

* Corresponding authors.
E-mail addresses: zhuangkunzk@163.com (K. Zhuang), whdingwp@163.com (W. Ding).
[1] Author contributed equally to this work

https://doi.org/10.1016/j.fochx.2025.102165
Received 4 November 2024; Received in revised form 24 December 2024; Accepted 6 January 2025
Available online 7 January 2025

nutritional enrichment during soaking and parboiling processes. Runge et al. (2019) examined the trace elements in brown rice, parboiled rice, and milled rice from the same brand available on the market. They found that the Se content in parboiled rice was higher than that in milled rice, while calcium, strontium and zinc exhibited greater sensitivity to the parboiling process. Conversely, Heinemann et al. (2005) reported that the Se content in parboiled rice and milled rice was essentially equivalent, yet the contribution of parboiled rice to the recommended dietary intake was greater than, milled rice.

During the literature search, it was noted that there are few comparative studies on the preparation of parboiled rice and milled rice from Se-enriched rice, as well as a lack of comprehensive evaluations regarding Se speciation, palatability, flavor, and other qualities. Therefore, the objectives of this work are to: (1) select three kinds of Se-enriched rice with varying selenium content to prepare both parboiled rice and milled rice; (2) investigate the effect of degree of milling on the Se content and hardness of the two rice products; (3) analyze the differences in Se speciation, textural properties of cooked rice, cooking quality, microstructure, taste, and flavor between the two products under reasonably well milled conditions.

2. Materials and methods

2.1. Raw materials

The three kinds of Se-enriched rice (*Oryza sativa L.*) utilized in this study are all Ezhong No. 6, supplied by the Hubei Academy of Agricultural Sciences (Wuhan, Hubei, China). The bio-selenium nanoparticles (bioSeNPs) fertilizers, produced by Hubei Academy of Agricultural Sciences (Wuhan, Hubei, China) with the size of nanoparticles ranging from 100 to 200 nm. During the heading stage, three concentrations of bioSeNPs fertilizers were applied to the rice leaves. The low-concentration of bioSeNps treatment (3.2 g Se/ha) is designated as R1 (total starch: 75.82 ± 0.63 %, total protein: 7.97 ± 0.12 %, amylose: 12.21 ± 0.52 %), the medium-concentration (6.4 g Se/ha) as R2 (total starch: 74.82 ± 0.79 %, total protein: 7.69 ± 0.09 %, amylose: 13.23 ± 0.23 %), and the high-concentration (19.3 g Se/ha) as R3 (total starch: 76.21 ± 0.29 %, total protein: 8.23 ± 0.04 %, amylose: 14.95 ± 0.48 %). The total selenium standard solution was obtained from the National Nonferrous Metal Analysis and Testing Center of China (Beijing, China), while the selenium species standard solution was provided by the China Institute of Metrology (Beijing, China). All remaining reagents were sourced from Sinopharm Chemical Reagent Co., Ltd. (Shanghai, China).

2.2. Preparation of parboiled rice and milled rice

Three appropriate levels were selected among the three factors, soaking temperature (40, 50, 60 °C), steaming time (25, 35, 45 min), and soaking time (4, 5, 6 h), a response surface experiment was designed with head rice rate as the response value, and a regression analysis was conducted (Fig. S1) to determine the optimal Se-enriched parboiled rice processing technology. Rice samples (200 g) were soaked in 50 mL of water at 50 °C for 4 h. According to the Approved Method (AACC 44–15.02, 2009), the measured moisture content is about 28 %, and then steamed for 20 min by rice steaming cabinet (LC-ZFG06, Nanjing Lechuang Kitchen Equipment Co., LTD., Nanjing, China). The sample was then spread flat on a tray and dried in a blast drying oven at 40 °C for 4 h until the moisture content reached 13 % to 14 %. During this drying period, the tray was removed every 30 min to allow the rice to cool at room temperature for 30 min, and this operation was repeated.

The dried rice samples were placed in sealed bags overnight, after which the rice husks were removed using a rice huller (JLG-II, China Grain Storage Chengdu Grain storage Research Institute, Chengdu, China). A 25 g sample of brown rice was weighed each time and ground in a laboratory-scale rice mill (BLH-3210, Zhejiang Bethlehem Instrument equipment Co., LTD, Hangzhou, China) for durations of 10s, 20s, 30s, 40s, 50s, and 60s, respectively. The three kinds of Se-enriched preboiled rice were respectively named: R1-P, R2-P, R3-P.

Se-enriched milled rice was obtained from unpreboiled grain by the same milling method and was named: R1-M, R2-M, R3-M.

2.3. Detection of degree of rice bran retention

The rice appearance inspection system (DMWG-01, Beijing Dongfu Jiuheng Instrument Technology Co., Ltd., Beijing, China) was utilized to assess the degree of bran retention in rice samples, with sample images subsequently scanned. In accordance with the operating manual, 12 g of the sample was weighed and placed into a Petri dish. An appropriate amount of deionized water was added to fully immerse the sample for 1 min, after which the bran powder was washed away and the clean water was discarded. Following the cleaning process, eosin *Y*-methyl blue dyeing solution was added to the sample for immersion; the mixture was shaken well and allowed to stand for 2 min before the dye was washed away. Subsequently, 80 % ethanol was added to submerge the rice grains, which were then shaken well and allowed to stand for 1 min before the liquid was poured out. This rinsing procedure was repeated three times to remove any excess dye. Immediately after rinsing, filter paper was used to absorb the remaining water from the sample, which was then allowed to dry naturally until no water stains were visible on the surface. The dried samples were placed into sealed bags and stored at room temperature until testing.

2.4. Texture profile analysis (TPA) of cooked rice

Wash the rice three times with distilled water. Weigh 10 g of the sample and add distilled water in a ratio of 1:1.3 into an aluminum box. Soak the rice for 10 min, then steam it under boiling water for 35 min, and keep it warm for an additional 10 min. The cooked rice had cooled at room temperature for 20 min.

The TPA of the cooked rice was performed using a texture analyzer (Rapid TA, Shanghai Tengba Instrument Technology Co., LTD, Shanghai, China) equipped with a P36/R Cylinder Probe, following the method described by (Tao et al., 2020) with minor modifications. Ten cooked rice kernels were evenly distributed in the center of the test bench, with a strain of 90 %. Five texture measurements were conducted for each sample.

2.5. Cooking quality

The parameters of rice cooking quality included water absorption (WA), starch-iodine blue (SIB) and cooking loss (CL). Follow (Zhao et al., 2024) method with slight modifications. Weigh 10 g of rice and mix it with 100 mL of distilled water in a beaker. After 20 min in a boiling water bath, separate the rice from the rice cooking liquid and record the weights of the sample before and after cooking. Dilute the rice cooking liquid to 100 mL with distilled water, centrifuge at 4000 r/min for 10 min, and dry the precipitate at 105 °C until a constant weight is achieved, then weigh it. Take 1 mL of the supernatant, and then add 1.0 mL of HCl (0.5 mol/L) and 1.0 mL of iodine reagent (0.2 mol/L). After that, dilute it to 100 mL with distilled water. Take 1 mL of the supernatant, 1.0 mL HCl (0.5 mol/L), 1.0 mL iodine reagent (0.2 mol/L) and dilute to 100 mL with distilled water. Use a spectrophotometer to measure the absorbance of the reaction solution at 600 nm, which corresponds to the iodine blue value of the rice cooking liquid.

$$WA = \frac{Weight\ of\ cooked\ rice - Weight\ of\ rice\ before\ cooking}{Weight\ of\ rice\ before\ cooking} \times 100 \quad (1)$$

$$CL = \frac{Weight\ of\ dried\ rice\ soup\ precipitate}{Weight\ of\ rice\ before\ cooking} \times 100 \quad (2)$$

2.6. Determination of total se content

The sample weighing 0.2 g ± 0.001 g and 7 mL of HNO_3 were placed in a digester tank and subjected to digestion in a microwave digester (W-8000, Shanghai Yiyao Instrument Technology Development Co., Ltd., Shanghai, China). Following digestion, the acid was evaporated at 200 °C until the solution volume was approximately 1 mL. After cooling to room temperature, 5 mL of 50 % HCl was added. The mixture was then heated at 180 °C for 20–30 s. Once cooled to room temperature, the volume was adjusted to 10 mL, and the total Se (T-Se) content of the sample was quantified using an atomic fluorescence spectrometer (LC-AFS8530, Beijing Haiguang Instrument Co., Ltd., Beijing, China). The carrier solution consisted of 10 % HCl, while the reduction solution was composed of 2 % KBH_4 and 0.35 % NaOH. Atomic fluorescence detection conditions were as follows: Se hollow cathode lamp with a total lamp current of 90 mA, secondary cathode current of 45 mA, argon as both the carrier and shielding gas at a pressure of 0.25 MPa, a negative voltage of 300 V on the photomultiplier tube, and a fluorescence intensity difference of 2000–3000.

2.7. Determination of se speciation

The method described in the literature (Sánchez-Martínez et al., 2015) was modified for this study. A total of 0.2 g ± 0.001 g of freeze-dried sample powder was placed in a 10 mL centrifuge tube and mixed with 5 mL of Tris-HCl buffer (75 mmoL, pH 7.5), along with 10 mg each of protease XIV and protease K. The mixture was shaken at 200 rpm for 12 h in a constant-temperature oscillation incubator maintained at 37 °C. Following this, centrifugation was performed at 10,000 rpm for 10 min, and the supernatant was filtered through a 0.22 μm hydrophilic filter membrane for analysis.

HPLC-ICP-MS (12900HPLC, 7800 ICP-MS, Agilent, Santa Clara, California, USA) was utilized to detect the form and content of Se. The Hamilton PRP-X100 chromatographic column (250 mm × 4.1 mm, 10 μm, Hamelton (Shanghai) Laboratory Equipment Co., Ltd., Shanghai, China) was employed to separate the test liquid. The HPLC flow rate was set at 1 mL·min^{-1}, with a sample injection volume of 10 μL, Radio-Frequency Power and Radio-Frequency Voltage was set 1480 W and 1.56 V, respectively. The sampling depth was set at 6.5 mm. The ICP-MS carrier flow rate was 1.1 mL·min^{-1}, the target detection element was ^{78}Se (m/z), the acquisition mode was set time resolution and Helium gas serves as the working gas in the collision/reaction cell of ICP-MS (He/He). Reference standard selenocompounds included selenocystine ($SeCys_2$), selenomethylcysteine (MeSeCys), selenomethionine (SeMet), selenite (Se IV) and selenate (Se VI). The retention times for $SeCys_2$, MeSeCys, SeMet, Se (VI) and Se (IV) were recorded as 136.08 s, 173.11 s, 294.17 s, 217.13 s, and 546.29 s, respectively (Fig. S2). The standard solution was mixture of five standard selenocompounds, the concentrations were 5, 10, 40, 80, 100 μg/L, respectively. The standard curve was constructed by plotting the peak areas against the corresponding concentrations of the five selenium standards. The retention times of the chromatographic peaks observed in the samples were compared with those of the standard substances to identify the selenium species. Quantitative analysis was performed based on the peak areas. The chromatograms of sample were provided in the Supplementary Material (Fig. S3).

For mobile phase preparation, 2 L of 20 mmoL citric acid monohydrate was prepared, the pH was adjusted to 4 using ammonia water, and 2 % methanol was incorporated (Mobile Phase A). Additionally, 1 L of 20 mmoL citric acid monohydrate was prepared, the pH was adjusted to 6 with ammonia water, and 1 % methanol was added (Mobile Phase B). Both mobile phases were filtered through a 0.22 μm hydrophilic filter membrane and subjected to ultrasound treatment for 30 min. The elution gradient program is as follows: From 0 to 2.5 min, the proportion of Mobile Phase A is 100 %, and the proportion of Mobile Phase B is 0 %. From 2.5 to 3.5 min, the proportion of Mobile Phase A changes to 0 %, and the proportion of Mobile Phase B changes to 100 %. From 3.5 to 6 min, Mobile Phase A remains at 0 %, and Mobile Phase B remains at 100 %. From 6 to 7 min, Mobile Phase A returns to 100 %, and Mobile Phase B returns to 0 %. From 7 to 12 min, Mobile Phase A continues to be 100 %, and Mobile Phase B continues to be 0 %.

2.8. Determination of relative crystallinity

The relative crystallinity of the sample was obtained with an X-ray diffractometer (D8-AdvanceX, Bruker, Germany) with Cu Kα radiation at 40 kV and 50 mA. The diffractograms were scanned between 5° and 40° (0.02°/2θ) at a rate of 1.2°/min. Relative crystallinity was estimated by the ratio of the peak areas to the total diffractogram area as described by referring to the method of (Li et al., 2021).

2.9. Determination of cross-section microstructure in cooked rice

Select whole grains of rice from the rice and use a freeze-dryer to remove water, then break them apart in the middle. Scanning electron microscopy (S-4700, HITACHI, Japan) was operated at 15 kV, 50 × and 250 × magnificaations. The rice cross section was observed at the 50-x, 250-x edge and 250-x center regions.

2.10. Determination of spatial distribution of starch and protein in cooked rice

The freeze-dried rice samples were cut into slices with a thickness of 15 μm using a freeze-microtome (CM-1950, Leica, Germany), and dyed with fluorescein isothiocyanate FITC (0.25 %, *w*/w) and Rhodamine B (0.025 %, w/w) for 10 min, and then washed with ultra-pure water. The 10× objective lens of CLSM (LSM-880, Carl ZeissAG, Germany) was used for observation. The images of protein (red) and starch (green) in rice were obtained by continuous scanning with different laser beams and emission filters, respectively. FITC and Rhodamine B are excited by lasers at 488 nm and 543 nm, respectively.

2.11. Analysis of taste characteristics of cooked rice

Take 50 g of cooked rice and 50 mL of pure water in a beaker. Homogenize the mixture for 2 min, then transfer the resulting slurry to a 50 mL centrifuge tube. Centrifuge the tube at 5000 rpm for 20 min. The supernatant obtained after centrifugation will be used to analyze taste characteristics using an electronic tongue (TS-5000Z, INSTENT, Fukuoka, Japan).

2.12. Analysis of flavor characteristics of cooked rice

Electronic nose (cNOSE-28, Bosin Industrial Development Co. Ltd., Shanghai, China) was used to detect volatile odors of cooked rice. The 28 Electronic Nose Sensor Configurations are shown in Table S2 of the Supplementary material. Take 5 g of cooked rice in a 20 mL headspace bottle, heat it in a metal bath at 80 °C for 30 min. The parameters were set as follows: injection flow rate of 0.4 L/min, test time of 80 s, and clean-up time of 120 s.

2.13. Statistics analysis

The data from three repeated experiments were analyzed to determine whether the variances were statistically homogeneous, and the results are expressed as the mean ± *SD*. The statistical comparisons were determined by one-way ANOVA followed by Duncan's multiple range test using SPSS (version 19.0, Statistical Package for the Social Sciences Inc., Chicago, USA). The differences were considered to be significant when the $P < 0.05$.

3. Results and discussion

3.1. Degree of milling on T-se content and hardness

Fig. 1a showed Degree of milling, T-Se content, and Hardness (cooked rice) of Se-enriched rice during milling. The processing precision of all samples increased significantly within the initial 40 s of milling, and then stabilized after 40 s. According to Chinese national standards (GB/T 5502–2018), the degree of milling is classified into three categories based on bran retention (Table S1): off-grade (10–20 s), reasonably well milled (20–40 s), and well milled (40–60 s), (Fig. 1a). Notably, the degree of milling for parboiled rice is consistently lower than that of milled rice at equivalen milling times. This is due to the greater difficulty in removing the bran from the back and germ portions of parboiled rice, as shown in Fig. 1b. After milling for 30 s, the bran retention of parboiled rice and milled rice was not different due to the difference of Se content (Table S1). This difficulty arises because steaming causes the oil in the rice bran to migrate outward, thereby increasing the milling resistance (Fellers & Deissinger, 1983). Additionally, parboiling densifies the grain structure and increases its strength, which ultimately reduces processing accuracy during milling (Gujral et al., 2002).

In contrast to the increase in processing accuracy, the total selenium (T-Se) content and hardness (cooked rice) of all samples gradually decreased (Fig. 1a), with samples exhibiting higher selenium content showing a more pronounced reduction of T-Se. Notably, the T-Se content across all samples stabilized after 40 s of milling, a finding consistent with the results reported by Liu et al. (2009). As indicated in Table S1, there is no statistically significant difference in the T-Se content between R1-P and R1-M ($P > 0.05$) However, the T-Se content in the parboiled rice of R2 and R3 is significantly higher than that of white rice ($P < 0.05$). This suggests that, at the same milling time, parboiled rice retains a greater T-Se content compared to milled rice. Previous studies have also found that the Se of parboiled milled rice is higher than milled rice (Runge et al., 2019). This phenomenon can be attributed to the higher retention of the bran in parboiled rice (Fig. 1b), where the concentration of Se was the highest in rice bran (Shen et al., 2019). Additionally, related studies indicate that during soaking, parboiled rice leaches water-soluble nutrients from the bran, and subsequent parboiling facilitates the transfer of these nutrients to the endosperm (Bhar et al., 2021). The cross-linking of gelatinized rice starch with micronutrients during the parboiling process significantly enhances the retention of these (Saha & Roy, 2020).Considering that Chinese consumers tend to prefer a softer cooked rice texture, this study focuses on the current trend of moderate processing. Samples milled for 40 s were selected to compare and analyze the differences between Se-enriched parboiled rice and Se-enriched milled rice.

3.2. Se speciation of parboiled and milled rice

The Se speciation of Se-enriched parboiled rice and Se-enriched milled rice, prepared by milling for 40 s, is presented in Fig. 2a. SeMet (72.6 %–80.1 %) is the main Se speciation. In comparison, the SeMet in parboiled rice consistently exceeds that in milled rice, which is reflected in the total amount of identified Se-species and T-Se content. When sodium selenite is applied to the leaves, approximately 80 % of the selenium in the harvested rice is found in organic form, with SeMet being the primary Se speciation that is readily absorbed (Wang et al., 2013). The Se(IV) is the main inorganic speciation of selenium (6.0 %–10.7 %). The R3 variety, which exhibits the highest selenium content, contains about 5 % of Se(VI) in both its parboiled and milled rice. Previous studies have indicated that the Se(VI) concentration in rice significantly increases following the application of selenium fertilizer during the booting stag (Huang et al., 2018). In this study, selenium fertilizer was applied during the heading stage, subsequent to the booting stage. Therefore, the concentration of Se(IV) is also higher than previously reported. In the low Se content R1 variety, unknown Se speciation constituted the highest proportion. The proportion of unknown Se species gradually decreased as the T-Se content increased, aligning with the results of previous research (Farooq, Zhang, Liu, et al., 2024; Farooq, Zhang, Yuan, et al., 2024).

3.3. Texture properties of cooked rice

The texture parameters in Table 1. There is no significant difference in hardness between R2-P and R2-M, R3-P and R3-M ($p > 0.05$). Overall,

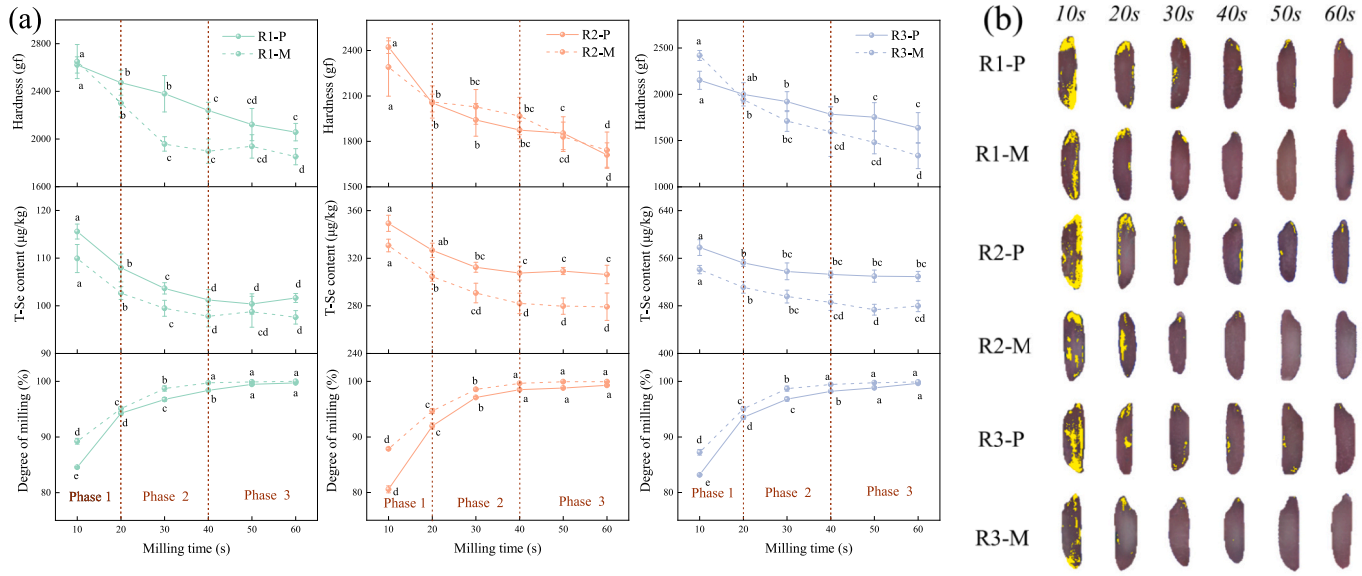

Fig. 1. The degree of milling, T-Se content and hardness of rice under different milling time (a): the figures are delineated into three categories of degree of milling by dotted lines, phase 1 is off-grade milled, phase 2 is reasonably well milled, phase 3 is well milled. The scanning image of rice bran retention under different milling time (b): the yellow area represents the bran on the surface of the rice grain. R1: the low-concentration of bioSeNps treatment of rice, R2: the medium-concentration of bioSeNps treatment of rice, R3: the high-concentration of bioSeNps treatment of rice, P: parboiled rice, M: milled rice. (For interpretation of the references to colour in this figure legend, the reader is referred to the web version of this article.)

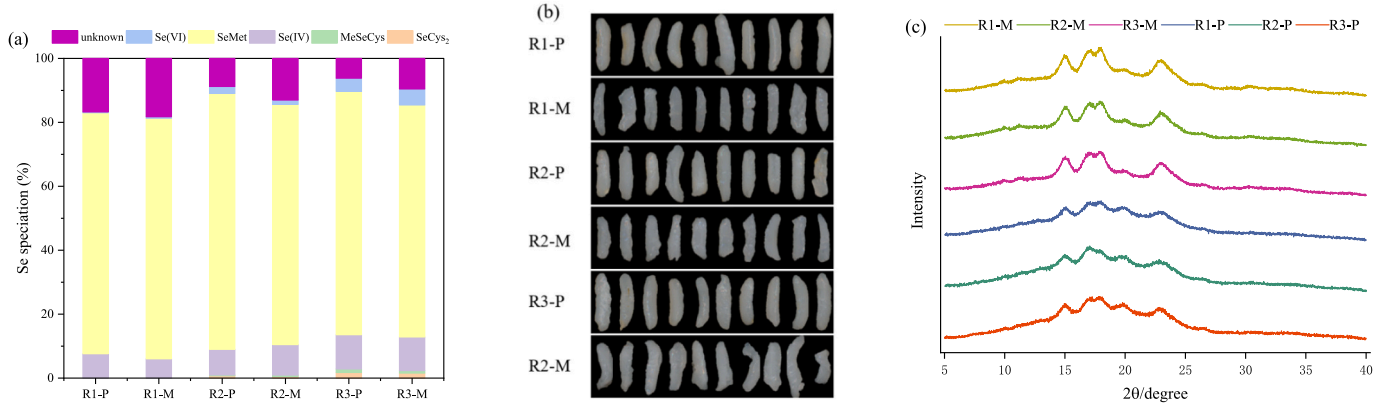

Fig. 2. Percentage of each Se speciation (a), the cooked rice contour image (b), XRD diffractogram of milled and parboiled rice (c) in the Se-enriched parboiled rice and Se-enriched milled rice. R1: the low-concentration of bioSeNps treatment of rice, R2: the medium-concentration of bioSeNps treatment of rice, R3: the high-concentration of bioSeNps treatment of rice, P: parboiled rice, M: milled rice.

Table 1
The texture properties and cooking quality of cooked rice.

Sample	Texture				Cooking quality		
	Hardness (gf)	Adhesiveness(gf•s)	Springiness	Chewiness (gf)	WA (%)	SIB	CL (%)
R1-P	2240.68 ± 68.09^{a}	−308.21 ± 50.44^{a}	0.633 ± 0.077^{b}	409.48 ± 19.41^{a}	249.92 ± 9.51^{b}	0.233 ± 0.006^{d}	1.19 ± 0.05^{d}
R1-M	1898.24 ± 102.19^{b}	−950.35 ± 67.08^{c}	0.383 ± 0.031^{c}	313.09 ± 17.02^{c}	281.00 ± 9.90^{a}	0.536 ± 0.006^{c}	2.15 ± 0.18^{b}
R2-P	1875.35 ± 57.48^{b}	−497.35 ± 42.03^{b}	0.796 ± 0.04^{a}	344.65 ± 16.02^{b}	248.6 ± 0.85^{b}	0.240 ± 0.013^{d}	1.45 ± 0.13^{cd}
R2-M	1967.42 ± 123.26^{b}	−1010.74 ± 31.65^{c}	0.342 ± 0.009^{c}	333.80 ± 13.65^{bc}	293.61 ± 9.90^{a}	0.598 ± 0.02^{b}	2.58 ± 0.05^{a}
R3-P	1784.08 ± 80.34^{bc}	−270.12 ± 17.7^{a}	0.796 ± 0.067^{a}	321.75 ± 4.98^{bc}	239.17 ± 2.72^{b}	0.278 ± 0.045^{d}	1.15 ± 0.14^{d}
R3-M	1596.7 ± 268.72^{c}	−951.52 ± 52.38^{c}	0.376 ± 0.038^{c}	318.42 ± 21.52^{bc}	260.61 ± 3.63^{b}	0.665 ± 0.008^{a}	2.18 ± 0.2^{b}

Note: Values with different letters are significantly different ($P < 0.05$). WA: water absorption, SIB: starch-iodine blue, CL: cooking loss, R1: the low-concentration of bioSeNps treatment of rice, R2: the medium-concentration of bioSeNps treatment of rice, R3: the high-concentration of bioSeNps treatment of rice, P: parboiled rice, M: milled rice.

parboiled rice has higher hardness and elasticity than milled rice, with less stickiness and similar chewiness. This can be attributed to the crystal structure formed by the gelatinization (steaming) and aging (drying) of starch in parboiled rice, which significantly influences its texture parameters (Li et al., 2021). The starch that dissolves during the cooking process accumulates on the surface of the rice grains, forming a mucous membrane that contributes to the adhesiveness (Yang et al., 2016). The hydrothermal treatment of parboiled rice leads to the formation of a dense microstructure within the particles, which affects the dissolution of starch during cooking (Jagtap et al., 2008), resulting in lower viscosity compared to milled rice.

Among the milled rice, no statistically significant differences were observed in the texture parameters of R1-M, R2-M, and R3-M. According to the study by Tao et al. (2020), although amylose content is correlated with hardness, the differences in amylose content among the three Se-enriched rice varieties (Section 2.1) are insufficient to significantly influence their hardness. Cheajesadagul et al. (2014) noted that selenium content may affect the activity of starch synthase, leading to differences in the content of amylose. R1-P possesses significantly higher hardness and chewiness compared to R2-P and R3-P, whereas its elasticity is markedly lower than those of the other two varieties. Additionally, R2-P demonstrated the highest adhesiveness among the parboiled rice samples. During the parboiling stage, starch gelatinizes and fills the micropores within the grains, enhancing the resistance of rice and affecting its hardness (Balbinoti et al., 2018). The parboiling process exerts a more substantial influence on the texture of cooked rice compared to selenium treatment. While chewiness is associated with hardness, there is no significant difference in chewiness between parboiled rice and milled rice for R2 and R3. Relevant research indicates that rice variety, processing method, and moisture content after parboiling can impact the textural properties of parboiled rice (Dutta et al., 2015).

3.4. Cooking qualities of cooked rice

Water absorption (WA), starch-iodine blue (SIB) and cooking loss (CL) are critical parameters that characterize the cooking quality of rice. The WA, SIB, and CL of Se-enriched parboiled rice from the three kinds were significantly lower than those of Se-enriched milled rice (Table 1). Rice cooking quality is primarily associated with changes in starch gelatinization (Tien et al., 2024). During cooking, the starch in rice gelatinizes due to heat, leading to dissolution, which allows water molecules to penetrate the starch particles more easily, causing the amorphous regions to hydrate and expand (Chakraborty et al., 2022). The parboiling process induces a degree of starch gelatinization in advance, and recrystallization during the drying process contributes to the dense internal structure of parboiled rice (Jagtap et al., 2008). This structural change affects the direction of water penetration during cooking. Consequently, the WA of parboiled rice is significantly lower than that of milled rice.

SIB reflects the degree of amylose dissolution in water during the cooking process, and highly correlated with CL (Tian et al., 2022), the results presented in Table 1 support this observation. Notably, the SIB for R1-M, R2-M, and R3-M were 0.536, 0.598, and 0.665, respectively, exhibiting a positive correlation with their amylose content (the amylose contents of R1, R2, and R3 are shown in Section 2.1). In contrast, the SIB and CL of parboiled rice showed no significant differences among varieties ($P > 0.05$), and both decreased by about half compared with milled rice. This indicates that parboiling limits starch dissolution during rice cooking, and this restriction is independent of amylose content. The phenomenon can be attributed to the gelatinization of starch on the surface of rice grains, which occurs due to steaming, thereby preventing starch leaching during cooking (Li et al., 2021). Additionally, the hydrothermal treatment enhances the strength of amylose-amylose and amylose-amylopectin interactions, which in turn

hinders their leaching from the rice particles (Tien et al., 2024).

This phenomenon can be observed more intuitively in Fig. 2b. The overall shape of the three types of parboiled cooked rice is more complete, and their surfaces are smoother. In contrast, milled cooked rice predominantly exhibits an open, cracked shape, with an irregular gel layer forming on its surface due to the adhesion of a greater quantity of dissolved substances. The amount of gel layer also significantly influences the stickiness of the rice (Li et al., 2019). Additionally, a small amount of rice peel remains on the surface of the parboiled rice, which corresponds to the processing accuracy depicted in Fig. 1a.

3.5. XRD patterns of parboiled and milled rice

Fig. 2c presents the XRD diffraction pattern of Se-enriched parboiled rice compared to milled rice. The diffraction pattern of milled rice reveals typical A-type starch crystals. In contrast, parboiled rice demonstrates a reduction in peak values at diffraction angles (2θ) of 15°, 17°, 18°, and 23°. This reduction is attributed to the parboiling process, which induces a certain degree of gelatinization in the starch, leading to partial melting of the crystalline regions (Sittipod & Shi, 2016). Relevant research showed the degree of starch gelatinization in parboiled rice is negatively correlated with both the crystallinity and stickiness of the rice (Patindol et al., 2008). Although the peak values for parboiled rice are diminished, there remains a distinct peak shape at the diffraction angles (2θ) of 15°, 17°, 18°, and 23°. According to the results (Li et al., 2021), the preparation method employed in this study restricts the extent of gelatinization in parboiled rice. Consequently, while the adhesiveness of parboiled rice is significantly reduced, its hardness and chewiness are comparable to those of white rice. In addition, despite the variation in selenium content among R1-P, R2-P, and R3-P, no significant differences were observed in their X-ray diffraction patterns. This implies that the impact of selenium concentration on the starch crystalline form of parboiled rice is substantially less than that caused by the starch pre-gelatinization due to parboiling treatment. It is also possible that the relatively low selenium levels in the samples, which are natural Se-enriched rice obtained through soil cultivation, are insufficient to induce a qualitative alteration in the starch structure.

3.6. SEM of cross-section of cooked rice

To investigate the differences in texture and cooking quality between Se-enriched parboiled rice and Se-enriched milled rice, scanning electron microscopy (SEM) was employed to observe the structural variations in the cross-section of the rice after freeze-drying. Fig. 3 a1-f1 illustrates the overall cross-section of the rice samples. The all samples exhibit a distinct depression at the center, surrounded by a pronounced porous structure. This porous architecture results from the sublimation of water within the rice during the freeze-drying process (Wu et al., 2016). The observed depression likely results from water migrating into the rice grains during cooking, combined with high temperatures that cause the grains to expand and form a cavity (Zhao et al., 2024). Consequently, this area is more susceptible to disconnection by external forces.

Fig. 3 a2-f2 presents an enlarged view of the edge of the rice section at 250 times magnification. It is observed that the porous structure gradually increases from the inside to the outside. During the cooking process, as starch gelatinizes, it penetrates outward to form a gel structure resembling a neural network. In contrast, the gel structure is less pronounced in parboiled rice. In milled rice, a distinct gel layer forms at the edge due to a higher concentration of dissolved matter (Nawaz et al., 2016). Fig. 3 a3-f3 shows an enlarged view of the center of the rice cross-section at the same magnification. The center of milled rice exhibits a significant number of microporous structures, and it is evident that the central area of R3-M (Fig. 3 e1) collapses and disintegrates, resulting in the formation of a thick gel layer at the edge of the rice grains from the dissolved gelatinized starch (Fig. 3 e2). This phenomenon accounts for the its high adhesiveness and low hardness. Conversely, the center of Se-enriched parboiled rice retains a solid structure and maintains an intact cell wall, resembling a honeycomb. This indicates that during the cooking process, only the starch in the peripheral region gelatinizes and dissolves. During the parboiling process, the pre-gelatinization and recrystallization of starch modify the internal structural stability of the rice grains. However, it is still unknown whether different selenium content samples will lead to structural differences between parboiled rice. Upon comparing Fig. 3 b3, d3, and f3, it is observed that the substantial center of R1-P exhibits the largest size, with R2-P being of secondary magnitude and R3-P the smallest, which also indicates that R1-P has the greatest hardness. Additionally, the number of pores, pore size, and gel thickness in Se-enriched milled rice are significantly greater than those in Se-enriched parboiled rice. The quantity and area of these pores can facilitate moisture transfer within the rice particles (Kumar et al., 2022), further illustrating the difficulty of water penetration into the interior of parboiled rice, which aligns with the WA results.

3.7. The spatial distribution of starch and protein in cooked rice

The spatial distribution differences of protein and starch in Se-enriched parboiled rice and Se-enriched milled rice were further examined using confocal laser scanning microscopy (CLSM) combined with fluorescent staining. Starch (green) and protein (red) in the rice were stained with fluorescein isothiocyanate (FITC) and rhodamine B, respectively. As illustrated in Fig. 4, the interior of milled rice has lost its complete starch granule shape. The dissolution of starch during gelatinization generates gaps, resulting in a looser structure (Fig. 4 a1, b1, c1). With continued cooking, the starch in the rice undergoes further gelatinization and dissolution, causing the starch granules to adhere to one another, making them difficult to distinguish (Chen et al., 2019). This gelatinized starch envelops the proteins that were originally located between the starch granules and migrates outward from within the milled rice (Zhu et al., 2020), forming a gel with a ground glass appearance (Fig. 4 a2, b2, c2). In contrast, the starch within parboiled rice retains part of its granular shape, exhibiting a relatively tighter structure (Fig. 4 d1, e1, f1). This observation indicates that, during the cooking of parboiled rice, further gelatinization and dissolution of starch is restricted. The protein (red) in the parboiled rice is still distributed within the starch gaps that maintain their granular shape (Fig. 4 d2, e2, f2), no red fluorescence is observed at the edges. The result showed that the dissolved substance of parboiled rice was basically starch and formed a gel layer on the surface of grains. The starch in milled rice is highly gelatinized, resulting in the dissolution of its granular morphology. The phenomenon further explains the difference in texture characteristics between parboiled rice and milled rice.

3.8. Taste characteristics of cooked rice

The electronic tongue was employed to analyze the taste profiles of each sample, encompassing the five basic tastes: sourness, bitterness, astringency, saltiness, and umami, as well as three aftertastes: aftertaste-A, aftertaste-B, and richness. Fig. 5a presents a radar chart depicting the taste response values for six samples. Notably, the sour and salty tastes exhibit negative values, indicating that they fall below the threshold of human taste perception. Thus, the changes in these two basic tastes will not be further discussed. Umami, which registers the highest response value, serves as the predominant flavor in Se-enriched parboiled rice and Se-enriched milled rice. Given the minimal differences in taste profiles among all samples (as indicated by the similar radar chart contours), a differential analysis was conducted using parboiled rice as the benchmark against milled rice. As shown in Fig. 5b, sample R1-M demonstrates a stronger astringency, whereas the taste changes of R2 and R3 post-parboiling are comparable (Fig. 5c and d). Overall, parboiled rice exhibited elevated levels of umami and richness, while the

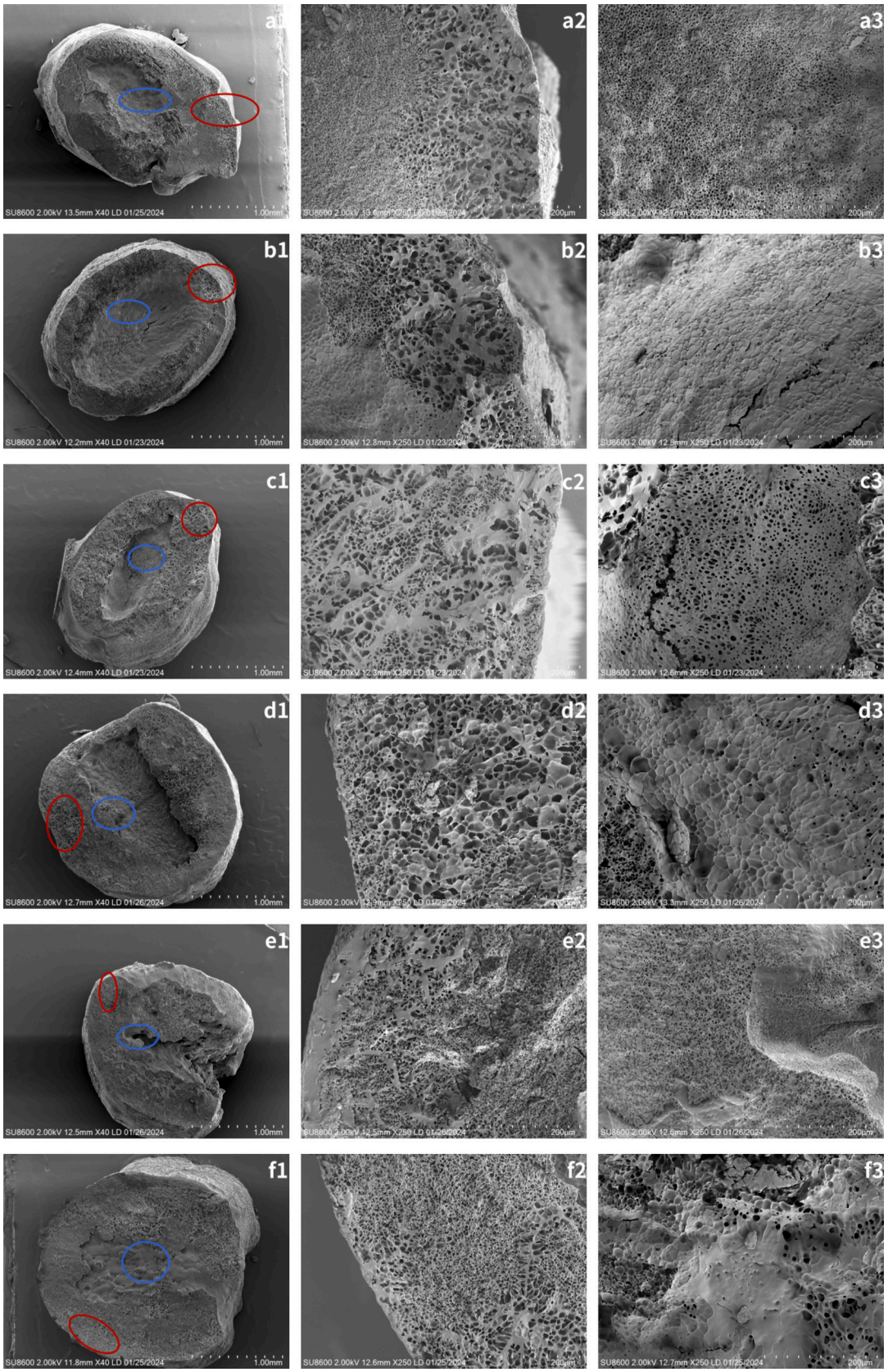

Fig. 3. SEM of Se-enriched parboiled rice and Se-enriched milled rice after cooking. R1-M (a), R1-P (b), R2-M (c), R2-P (d), R3-M(e), R3-P (f), cross-section (1), centeral area (red circle) (2), central area (bule circle) (3). R1: the low-concentration of bioSeNps treatment of rice, R2: the medium-concentration of bioSeNps treatment of rice, R3: the high-concentration of bioSeNps treatment of rice, P: parboiled rice, M: milled rice. (For interpretation of the references to colour in this figure legend, the reader is referred to the web version of this article.)

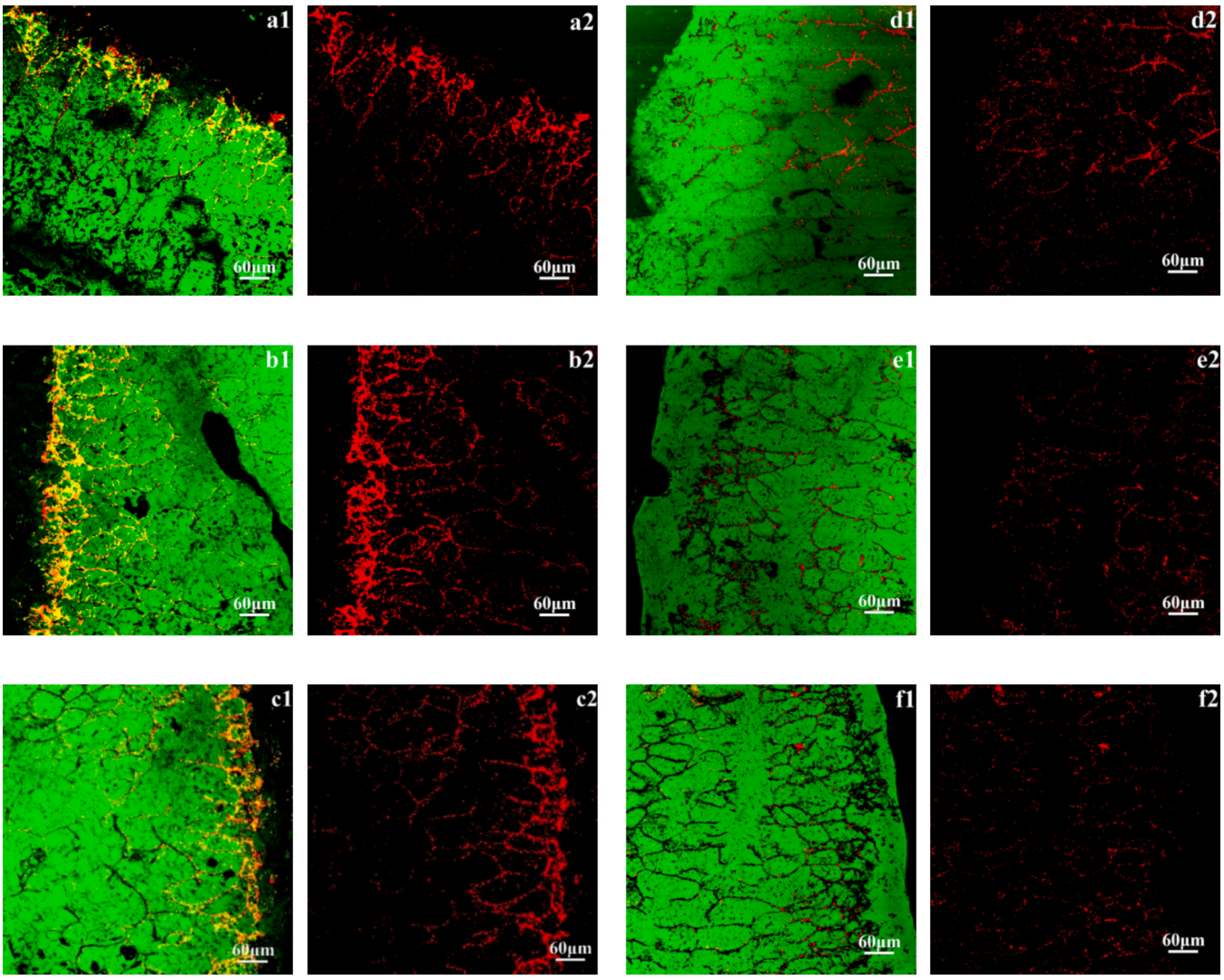

Fig. 4. CLSM of Se-enriched parboiled rice and Se-enriched milled rice after cooking. R1-M (a), R2-M (b), R3-M (c), R1-P (d), R2-P(e), R3-P (f), the gluten was stained by Rhodamine B (1, red), the starch was stained by FITC (2, green). R1: the low-concentration of bioSeNps treatment of rice, R2: the medium-concentration of bioSeNps treatment of rice, R3: the high-concentration of bioSeNps treatment of rice, P: parboiled rice, M: milled rice. (For interpretation of the references to colour in this figure legend, the reader is referred to the web version of this article.)

increase in bitterness did not alter aftertaste-B. This enhancement in bitterness may be attributed to the enrichment of nutrients such as phenolics (Mudgal & Singh, 2024). Previous studies have also indicated that parboiled rice enhances both umami and saltiness, contributing to a more pleasant and satisfying flavor experience (Huang et al., 2021).

3.9. Flavor characteristics of cooked rice

Fig. 6a illustrates that the electronic nose radar map profiles of all samples exhibit similarities; however, there are notable differences in the response values to the sensors. In comparison to milled rice, the radar chart area for parboiled rice has increased, indicating parboiled rice possesses a richer flavor. Nevertheless, the parboiling process does not alter the overall flavor structure of the rice. In the PCA score (Fig. 6b), the contribution rate of PC1 is 55.7 %, while that of PC2 is 21.7 %. The cumulative contribution exceeds 75 %, effectively representing the majority of the sample information. The spatial distribution of all sample points has been effectively separated, with R1-M, R2-M, and R3-M located in three distinct areas. Conversely, R1-P, R2-P, and R3-P progressively converge toward the center of the figure, indicating a consistent directional change in the flavor of cooked rice influenced by the parboiling process. The overlapping radar curves of the three types of selenium-rich parboiled rice in Fig. 6a further corroborate these findings. Additionally, when combined with the PCA double plot (Fig. 6c), the scattering behavior of the samples reveals the sensors with the most pronounced responses (Ma et al., 2023). The response values for parboiled rice in sensors S5, S9, S11, S12, S14, S19, S23, and S26 demonstrate significant improvement. According to the descriptions of the response materials for each sensor provided in Table S2, the processing of parboiled rice enhances the presence of various compounds, including ammonia compounds, aldehydes, ketones, short-chain alkanes, esters, aliphatic hydrocarbons, aromatic hydrocarbons, volatile organic compounds, sulfides.

4. Conclusions

In this work, parboiled rice and milled rice were produced by applying three distinct concentrations of bioSeNPs fertilizer to the leaves of Se-enriched rice during the heading stage. Under reasonably well milled, evidence was presented demonstrating significant differences in Se speciation, textural properties of cooked rice, cooking quality, microstructure, taste and flavor between the two products. The

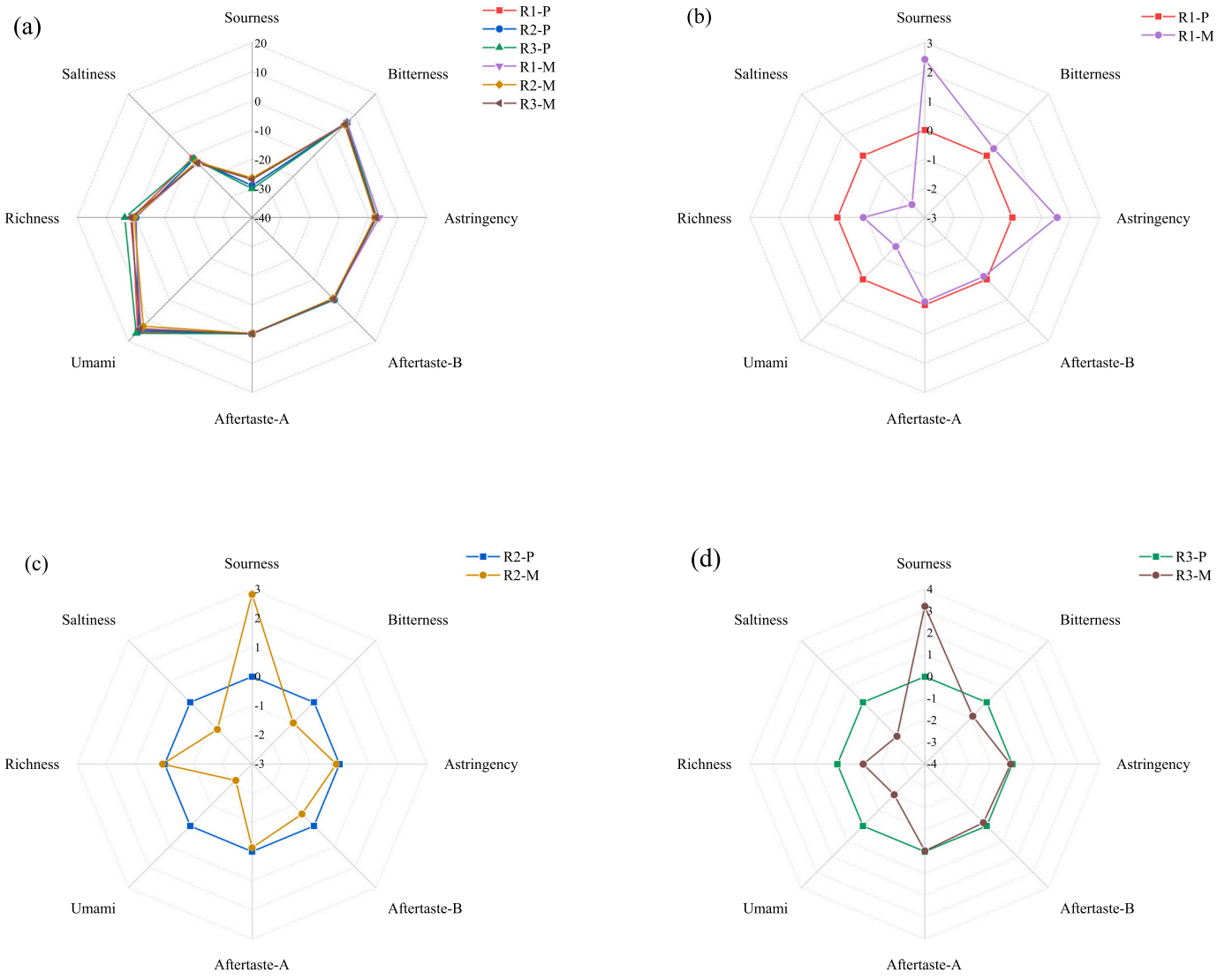

Fig. 5. Electronic tongue radar diagram of Se-enriched parboiled rice and Se-enriched milled rice after cooking. Six samples were not differentially analyzed (a), R1-P (standard) and R1-M difference analysis (b), R2-P (standard) and R2-M difference analysis (c), R3-P (standard) and R3-M difference analysis (d). Aftertaste-B: Bitterness aftertaste, Aftertaste-A: Astringency aftertaste, Richness: Umami aftertaste, R1: the low-concentration of bioSeNps treatment of rice, R2: the medium-concentration of bioSeNps treatment of rice, R3: the high-concentration of bioSeNps treatment of rice, P: parboiled rice, M: milled rice.

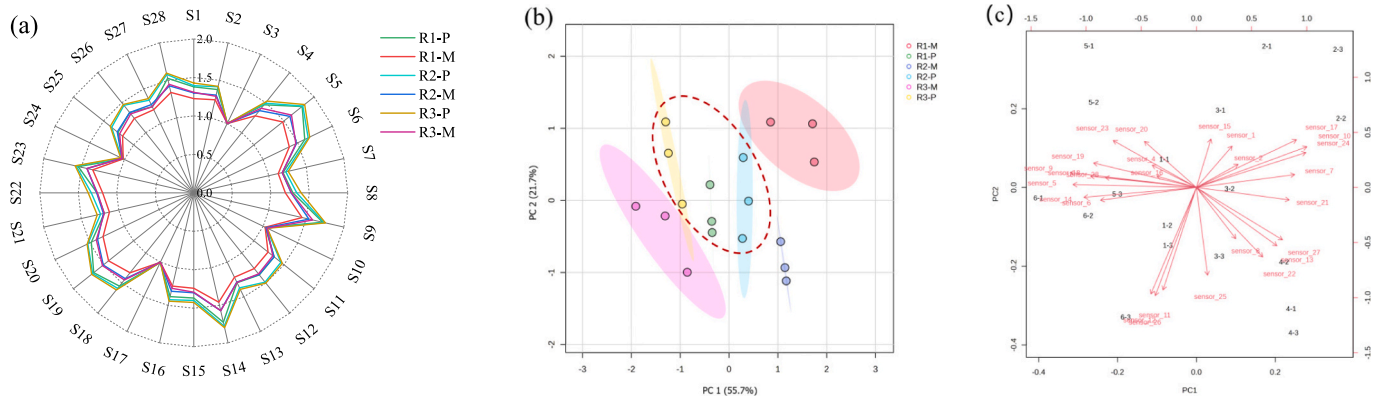

Fig. 6. Electronic nose radar diagram of Se-enriched parboiled rice and Se-enriched milled rice after cooking (a), Principal component analysis (PCA) score plot (b), PCA biplot (c). R1: the low-concentration of bioSeNps treatment of rice, R2: the medium-concentration of bioSeNps treatment of rice, R3: the high-concentration of bioSeNps treatment of rice, P: parboiled rice, M: milled rice.

proportion of selenoamino acids in all samples ranged from 80.1 % to 88.3 %, with parboiled rice of the same kind exhibiting higher levels than milled rice. R1-P displayed the highest hardness and chewability; however, no statistically significant differences were observed among other samples ($p > 0.05$). Results from cooking quality, along with SEM and CLSM indicated that pre-gelatinization of parboiled rice hinders water absorption during cooking, thereby limiting starch dissolution post-gelatinization. Consequently, the adhesiveness of parboiled rice was significantly lower than that of milled rice ($p < 0.05$). The taste and flavor profiles of the three kinds of Se-enriched rice exhibited similar trends following parboiling. Notably, the observed differences in cooked rice indicators are primarily attributed to parboiling, rather than the T-Se content or amylose content of themselves. These findings provide valuable insights for processing and application strategies concerning Se-enriched rice.

CRediT authorship contribution statement

Kun Zhuang: Writing – review & editing, Writing – original draft, Supervision, Resources, Methodology, Funding acquisition, Conceptualization. **Zihan Zhang:** Writing – original draft, Software, Methodology, Investigation, Data curation. **Shuyou Shang:** Methodology, Investigation, Data curation. **Kai Zheng:** Methodology, Investigation. **Xiaolong Zhou:** Methodology, Investigation. **Wenjing Huang:** Methodology, Investigation. **Yuehui Wang:** Writing – original draft, Supervision. **Wenping Ding:** Writing – review & editing, Funding acquisition, Conceptualization.

Declaration of competing interest

The authors declare that they have no known competing financial interests or personal relationships that could have appeared to influence the work reported in this paper.

Acknowledgements

This research was funded by the Hubei Province key research and development project [No. 2023BBB146], National Key Research and Development Program of China [No. 2023YFF1104600] and the Central Government Guides Local Science and Technology Development Projects [No. 2022BGE247].

Appendix A. Supplementary data

Supplementary data to this article can be found online at https://doi.org/10.1016/j.fochx.2025.102165.

Data availability

No data was used for the research described in the article.

References

Balbinoti, T. C. V., Nicolin, D. J., de Matos Jorge, L. M., & Jorge, R. M. M. (2018). Parboiled Rice and parboiling process. *Food Engineering Reviews, 10*(3), 165–185. https://doi.org/10.1007/s12393-018-9177-y

Bhar, S., Bose, T., Dutta, A., & Mande, S. S. (2021). A perspective on the benefits of consumption of parboiled rice over brown rice for glycaemic control. *European Journal of Nutrition, 61*(2), 615–624. https://doi.org/10.1007/s00394-021-02694-x

Chakraborty, I. N. P., Mal, S. S., Paul, U. C., Rahman, M. H., & Mazumder, N. (2022). An insight into the gelatinization properties influencing the modified starches used in food industry: A review. *Food and Bioprocess Technology, 15*(6), 1195–1223. https://doi.org/10.1007/s11947-022-02761-z

Cheajesadagul, P., Bianga, J., Arnaudguilhem, C., Lobinski, R., & Szpunar, J. (2014). Large-scale speciation of selenium in rice proteins using ICP-MS assisted electrospray MS/MS proteomics. *Metallomics, 6*(3), 646–653. https://doi.org/10.1039/c3mt00299c

Chen, X., Zhang, X., Wang, B., Chen, P., Xu, Y., & Du, X. (2019). Investigation of water migration and its impacts on eating qualities of black rice during cooking process. *Journal of Cereal Science, 89*. https://doi.org/10.1016/j.jcs.2019.102810

Dutta, H., Mahanta, C. L., & Singh, V. (2015). Changes in the properties of rice varieties with different amylose content on dry heat parboiling. *Journal of Cereal Science, 65*, 227–235. https://doi.org/10.1016/j.jcs.2015.07.016

Farooq, M. R., Zhang, Z., Yuan, L., Liu, X., Li, M., Song, J., … Yin, X. (2024). Characterization of selenium speciation in Se-enriched crops: Crop selection approach. *Journal of Agricultural and Food Chemistry, 72*(7), 3388–3396. https://doi.org/10.1021/acs.jafc.3c08116

Farooq, M. R., Zhang, Z. Z., Liu, X. D., Chen, Y. T., Wu, G. G., Niu, S. S., … Yin, X. B. (2024). Selenium loss during boiling processes and its bioaccessibility in different crops: Estimated daily intake. *Food Chemistry, 443*. https://doi.org/10.1016/j.foodchem.2024.138607

Fellers, D. A., & Deissinger, A. E. (1983). Preliminary study on the effect of steam treatment of rice paddy on milling properties and rice stickiness. *Journal of Cereal Science, 1*(2), 147–157. https://doi.org/10.1016/s0733-5210(83)80032-0

Gujral, H. S., Singh, J., Sodhi, N. S., & Singh, N. (2002). Effect of milling variables on the degree of milling of Unparboiled and parboiled Rice. *International Journal of Food Properties, 5*(1), 193–204. https://doi.org/10.1081/jfp-120015601

Heinemann, R. J. B., Fagundes, P. L., Pinto, E. A., Penteado, M. V. C., & Lanfer-Marquez, U. M. (2005). Comparative study of nutrient composition of commercial brown, parboiled and milled rice from Brazil. *Journal of Food Composition and Analysis, 18*(4), 287–296. https://doi.org/10.1016/j.jfca.2004.07.005

Huang, G., Ding, C., Yu, X., Yang, Z., Zhang, T., & Wang, X. (2018). Characteristics of time-dependent selenium biofortification of Rice (*Oryza sativa* L.). *Journal of Agricultural and Food Chemistry, 66*(47), 12490–12497. https://doi.org/10.1021/acs.jafc.8b04502

Huang, W., Song, E., Lee, D., Seo, S., Lee, J., Jeong, J., Chang, Y.-H., Lee, Y.-M., & Hwang, J. (2021). Characteristics of functional brown rice prepared by parboiling and microwave drying. *Journal of Stored Products Research, 92*. https://doi.org/10.1016/j.jspr.2021.101796

Jagtap, P. S., Subramanian, R., & Singh, V. (2008). Influence of soaking on crushing strength of raw and parboiled Rice. *International Journal of Food Properties, 11*(1), 127–136. https://doi.org/10.1080/10942910701272320

Kumar, A., Lal, M. K., Nayak, S., Sahoo, U., Behera, A., Bagchi, T. B., … Sharma, S. (2022). Effect of parboiling on starch digestibility and mineral bioavailability in rice (*Oryza sativa* L.). *Lwt, 156*. https://doi.org/10.1016/j.lwt.2021.113026

Li, H., Yan, S., Yang, L., Xu, M., Ji, J., Mao, H., Song, Y., Wang, J., & Sun, B. (2021). Starch gelatinization in the surface layer of rice grains is crucial in reducing the stickiness of parboiled rice. *Food Chemistry, 341*(Part 2), Article 128202. https://doi.org/10.1016/j.foodchem.2020.128202

Li, H., Yang, J., Gao, M., Wang, J., & Sun, B. (2019). Washing rice before cooking has no large effect on the texture of cooked rice. *Food Chemistry, 271*(0), 388–392. https://doi.org/10.1016/j.foodchem.2018.07.172

Liu, K., Cao, X., Bai, Q., Wen, H., & Gu, Z. (2009). Relationships between physical properties of brown rice and degree of milling and loss of selenium. *Journal of Food Engineering, 94*(1), 69–74. https://doi.org/10.1016/j.jfoodeng.2009.03.001

Ma, Y., Yin, J. J., Wang, J. Y., Liu, X., He, J. R., Zhang, R., … Wu, M. C. (2023). Selenium speciation and volatile flavor compound profiles in the edible flowers, stems, and leaves of selenium-hyperaccumulating vegetable Cardamine violifolia. *Food Chemistry, 427*. https://doi.org/10.1016/j.foodchem.2023.136710

Muchlisyiyah, J., Shamsudin, R., Kadir Basha, R., Shukri, R., How, S., Niranjan, K., & Onwude, D. (2023). Parboiled rice processing method, rice quality, health benefits, environment, and future perspectives: A review. *Agriculture, 13*(7), 1390.

Mudgal, S., & Singh, N. (2024). Effect of parboiling treatment times on the physicochemical, cooking, textural, and pasting properties and amino acid, phenolic, and sugar profiles of germinated paddy rice from different rice varieties. *Journal of Food Science, 89*(6), 3208–3229. https://doi.org/10.1111/1750-3841.17048

Muleya, M., Young, S. D., Reina, S. V., Ligowe, I. S., Broadley, M. R., Joy, E. J. M., … Bailey, E. H. (2021). Selenium speciation and bioaccessibility in Se-fertilised crops of dietary importance in Malawi. *Journal of Food Composition and Analysis, 98*. https://doi.org/10.1016/j.jfca.2021.103841

Nawaz, M. A., Gaiani, C., Fukai, S., & Bhandari, B. (2016). X-ray photoelectron spectroscopic analysis of rice kernels and flours: Measurement of surface chemical composition. *Food Chemistry, 212*, 349–357. https://doi.org/10.1016/j.foodchem.2016.05.188

Patindol, J., Newton, J., & Wang, Y. J. (2008). Functional properties as affected by laboratory-scale parboiling of rough Rice and Brown Rice. *Journal of Food Science, 73*(8), E370–E377. https://doi.org/10.1111/j.1750-3841.2008.00926.x

Runge, J., Heringer, O. A., Ribeiro, J. S., & Biazati, L. B. (2019). Multi-element rice grains analysis by ICP OES and classification by processing types. *Food Chemistry, 271*, 419–424. https://doi.org/10.1016/j.foodchem.2018.07.162

Saha, S., & Roy, A. (2020). Whole grain rice fortification as a solution to micronutrient deficiency: Technologies and need for more viable alternatives. *Food Chemistry, 326*. https://doi.org/10.1016/j.foodchem.2020.127049

Sánchez-Martínez, M., Pérez-Corona, T., Cámara, C., & Madrid, Y. (2015). Preparation and characterization of a laboratory scale Selenomethionine-enriched bread. Selenium bioaccessibility. *Journal of Agricultural and Food Chemistry, 63*(1), 120–127. https://doi.org/10.1021/jf505069d

Shen, J., Jiang, C., Yan, Y., & Zu, C. (2019). Selenium distribution and translocation in Rice (*Oryza sativa* L.) under different naturally Seleniferous soils. *Sustainability, 11*(2). https://doi.org/10.3390/su11020520

Sittipod, S., & Shi, Y.-C. (2016). Changes of starch during parboiling of rice kernels. *Journal of Cereal Science, 69*, 238–244. https://doi.org/10.1016/j.jcs.2016.03.015

Tao, K., Yu, W., Prakash, S., & Gilbert, R. G. (2020). Investigating cooked rice textural properties by instrumental measurements. *Food Science and Human Wellness, 9*(2), 130–135. https://doi.org/10.1016/j.fshw.2020.02.001

Tian, X. H., Tan, B., Wang, L. X., Zhai, X. T., Jiang, P., Qiao, C. C., & Wu, N. N. (2022). Effect of rice bran with extrusion cooking on quality and starch retrogradation of fresh brown rice noodles during storage at different temperatures. *Cereal Chemistry, 99*(6), 1296–1307. https://doi.org/10.1002/cche.10592

Tien, N. N. T., Phi, N. T. L., Thu, N. N. A., Oanh, T. T. H., & Van Hung, P. (2024). Cooking quality, textural characteristics and sensory evaluation of heat-moisture treated unpolished red rice under different cooking conditions. *International Journal of Food Science & Technology, 1*. https://doi.org/10.1111/ijfs.16913

Wang, Y.-D., Wang, X., & Wong, Y.-S. (2013). Generation of selenium-enriched rice with enhanced grain yield, selenium content and bioavailability through fertilisation with selenite. *Food Chemistry, 141*(3), 2385–2393. https://doi.org/10.1016/j.foodchem.2013.05.095

White, P. J. (2018). Selenium metabolism in plants. *Biochimica et Biophysica Acta-General Subjects, 1862*(11), 2333–2342. https://doi.org/10.1016/j.bbagen.2018.05.006

Wu, J., Chen, J., Liu, W., Liu, C., Zhong, Y., Luo, D., Li, Z., & Guo, X. (2016). Effects of aleurone layer on rice cooking: A histological investigation. *Food Chemistry, 191*, 28–35. https://doi.org/10.1016/j.foodchem.2014.11.058

Wu, X., Guo, T., Luo, F., & Lin, Q. (2023). Brown rice: A missing nutrient-rich health food. *Food Science and Human Wellness, 12*(5), 1458–1470.

Xiong, Y., Tian, X. H., Qiu, T. C., Cong, X., Zheng, X. F., Chen, S. Y., … Xu, D. Z. (2023). Effects of SeNPs fertilizer on se and microelement contents, eating and cooking qualities, and volatile organic compounds in Rice grains. *Sustainability, 15*(13). https://doi.org/10.3390/su151310553

Yang, L., Sun, Y.-H., Liu, Y., Mao, Q., You, L.-X., Hou, J.-M., & Ashraf, M. A. (2016). Effects of leached amylose and amylopectin in Rice cooking Liquidon texture and structure of cooked Rice. *Brazilian Archives of Biology and Technology, 59*(spe). https://doi.org/10.1590/1678-4324-2016160504

Zhao, S. S., Shi, J. B., Cai, S., Xiong, T., Cai, F., Li, S. B., … Sui, Y. (2024). Impact of rice variety, cooking equipment and pretreatment method on the quality of lightly milled rice. *Food Chemistry, 451*. https://doi.org/10.1016/j.foodchem.2024.139271

Zhu, L., Wu, G., Cheng, L., Zhang, H., Wang, L., Qian, H., & Qi, X. (2020). Investigation on molecular and morphology changes of protein and starch in rice kernel during cooking. *Food Chemistry, 316*. https://doi.org/10.1016/j.foodchem.2020.126262